Geomechanics and Engineering, *Vol. 36, No. 1 (2024) 71-81*
https://doi.org/10.12989/gae.2024.36.1.071

Assessment of pull-out behavior of tunnel-type anchorages under various joint conditions

Junyoung Ko[1], Hyunsung Lim[2], Seunghwan Seo[3] and Moonkyung Chung*[3]

[1]*Department of Civil Engineering, Chungnam National University, Daejeon 34134, Republic of Korea*
[2]*Department of Wind Power Business, Hanwha Corporation/E&C, 86, Cheonggyecheon-ro, Jung-gu, Seoul, 04541, Republic of Korea*
[3]*Department of Geotechnical Engineering Research, Korea Institute of Civil Engineering and Building Technology, Goyang-si, Gyeonggi-do 10223, Republic of Korea*

(*Received May 15, 2023, Revised November 27, 2023, Accepted December 4, 2023*)

Abstract. This study analyzes the pull-out behavior of tunnel-type anchorage under various joint conditions, including joint direction, spacing, and position, using a finite element analysis. The validity of the numerical model was evaluated by comparing the results with a small-scaled model test, and the results of the numerical analysis and the small-scaled model test agree very well. The parametric study evaluated the quantitative effects of each influencing factor, such as joint direction, spacing, and position, on the behavior of tunnel-type anchorage using pull-out resistance-displacement curves. The study found that joint direction had a significant effect on the behavior of tunnel-type anchorage, and the pull-out resistance decreased as the displacement level increased from 0.002*L* to 0.006*L* (*L*: anchorage length). It was confirmed that the reduction in pull-out resistance increased as the number of joints in contact with the anchorage body increased and the spacing between the joints decreased. The pull-out behavior of tunnel-type anchorage was thus shown to be significantly influenced by the position and spacing of the rock joints. In addition, it is found that the number of joints through which the anchorage passes, the wider the area where the plastic point occurs, which leads to a decrease in the resistance of the anchorage.

Keywords: finite element analysis; pull-out resistance; rock joint conditions; suspension bridge; tunnel-type anchorage

1. Introduction

In a suspension bridge, the deck hangs below suspension cables with both ends fixed, supporting the weight imparted to the bridge with the tensile force of the cables. Due to its significant benefits in terms of material qualities and the height-spans ratio of the stiffening girder, it is a commonly utilized long-span bridge construction. (Lekidis *et al.* 2005, Gwon and Choi 2018, Han *et al.* 2019).

Suspension bridges can be earth-anchored or self-anchored, depending on the method employed to attach the main cable (Deng *et al.* 2018). In contrast to earth-anchored suspension bridges, which fix the main cable by deploying anchorages at both ends of the bridge, self-anchored suspension bridges attach the main cable by installing anchorages on the pier at the end of the bridge. Because a significant load is exerted when fastening the main cables, the anchorage of earth-anchored suspension bridges is essential for preserving the stability of the entire structure. Gravity-type, tunnel-type, and rock-anchored anchorages are the three main categories of anchorages (Li and Li 2006, Han *et al.* 2019, Lim *et al.* 2020, 2021, 2022, Seo *et al.* 2021).

Because the anchorage's self-weight supports the cable load, gravity-type anchorages may be employed regardless of the condition of the ground. These anchorages also require a lot of concrete and a lot of construction space. The ground must be dug up, and a tunnel filled with steel and concrete must be filled in order to support the cable weight of the bridge (ASCE 1979, Dakeuchi and Yoshida 1984, Hong *et al.* 2014,). Tunnel-type anchorages have a good performance-cost ratio and rarely cause environmental disruption (Fig. 1). From the perspective of space and environmental issues, the tunnel-type anchorage may be preferred. Tunnel-type anchorages should be taken into consideration when site circumstances are acceptable, according to the Design Specifications for Highway Suspension Bridges (Lei *et al.* 2012). The primary cable tension and supporting load of the anchorage grow as the suspended span length of cable supported bridges rises. Consequently, the volume of the anchoring also grows. If the ground conditions, such as hard rock or soft rock, are met, tunnel-type anchorage should be used utilizing solid ground. Under stiff ground conditions, the tunnel-type anchorage can hold a weight that is 20–25 percent more than the gravity-type anchorage (Zhang *et al.* 2015, Han *et al.* 2019).

Tunnel-type anchorages are more subject to the condition of the ground than gravity-type anchorages are. The geometry of the cross-section of the anchorage and the characteristics of the surrounding rock, in particular, affect the mechanism of collapse. Throughout the design phase, the failure mechanism is evaluated and the pull-out resistance and stability are examined at in relation to the characteristics of the surrounding rock mass and the cross-sectional shape of the anchorage. Conservative failure

*Corresponding author, Ph.D.
E-mail: mkchung@kict.re.kr

ISSN: 2005-307X (Print), 2092-6219 (Online)

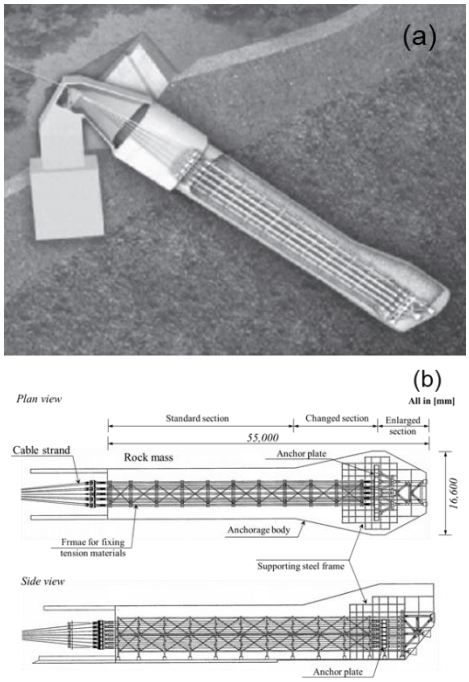

Fig. 1 Typical shape of tunnel-type anchorage: (a) schematic diagram and (b) plan view and side view (Yooshin Co., Ltd. 2009)

scenarios have been used to design tunnel-type anchorages in common applications (Park *et al.* 2009). Collapse mechanisms are frequently observed to happen along the boundary surface of the surrounding rock mass parallel to the direction of the anchor force rather than emerging as a spread or wedge failure (Park *et al.* 2013, Park *et al.* 2014). At the surface of the anchorage body, the failure surface develops in an axial direction. However, it should really be predicted that a wedge-shaped collapse will take place when a load is exerted to the ground in the axial and radial directions of the enlarged section, pressing the surrounding ground together (Kanemitsu *et al.* 1980).

Tunnel-type anchorages are rarely utilized in design, and it is yet unknown how they will react to a pull-out load. The mechanical aspects of tunnel-type anchorages are close to those of uplift piles and rock anchors (Han *et al.* 2019). The mechanical behavior of uplift piles has been studied using a variety of model experiments and numerical simulations (Aydan *et al.* 1993, Alawneh *et al.* 1999, Ilamparuthi *et al.* 2002, Shanker *et al.* 2007, Han *et al.* 2019). However, it is challenging to correlate the failure mode of the uplift pile to the failure mode of anchorage since the structures differ in shape, size, and material. Additionally, the failure mechanism of tunnel-type anchorages is affected by the presence of discontinuities, such as joints and artificial and naturally occurring faults (Han *et al.* 2019). However, there hasn't been much research on the shape and characteristics of rock joints in connection to tunnel-type anchorages.

In this study, pull-out behavior of tunnel-type anchorage investigated according to rock joint characteristics using 3D finite element analysis. Numerical solutions were verified against data from small-scaled model test conducted in previous studies (Seo *et al.* 2018, 2021). The major influencing factors, i.e., joint direction, spacing, and position on the tunnel-type anchorage response are analyzed.

2. Problem definition

In the tunnel-type anchorage for suspension bridge, the anchorage sphere is formed by excavating a tunnel in the ground, embedding a steel frame to fix the main cable in the excavation, and then pouring concrete. That is, it is supported by the self-weight of the concrete sphere inside the tunnel and the friction and adhesion resistance of the original ground in contact with the concrete sphere.

For the optimal design of tunnel-type anchorages, it should analyze the strength of the supported rock, the characteristics of discontinuities, the shape of the anchorage, etc., and calculates the pull-out resistance based on the failure angle reasonably assumed. Although the design of tunnel-type anchorage in Korea assumes that the failure surface is linearly distributed along the axial outer surface of the anchorage sphere, the criteria for this method are not clear. In addition, the range of relaxation and damage to the rock and its strength due to tunnel excavation are not clearly established as criteria. Because the tunnel-type anchorage is a structure significantly affected by the rock characteristics such as strengths and discontinuities (i.e., rock joints), therefore, it is necessary to analyze the anchorage behavior and failure patterns according to those. In particular, the quantitative results on the behavior of tunnel-type anchorages according to the influence of the joint characteristics are required at the design stage, and it will be practically helpful in the design.

In this study, a series of 3D finite element analyses were performed to analyze the pull-out behavior of tunnel-type anchorages according to the direction, spacing and position of the joints in the rock which the anchorage was installed. Fig. 2 shows the definition and key parameters of the problem. Fig. 2(a) illustrates a schematic diagram for analyzing the effect of the direction of the rock joint. It is assumed that the x-axis and y-axis exist on the surface of the joint, and the direction is defined as the angles between the direction of the applied load on anchorage and x- and y-axis, respectively. In other words, it is defined as the angle i_y between the load direction and y-axis on the joint, and angle i_x between the load direction and x-axis on the joint, respectively. To investigate the anchorage behavior according to directions of rock joints, cases 1 - 4 were fixed as $i_y = 90°$ with varying $i_x = 0°$, 30°, 60°, and 90° and cases 5 - 9 were fixed as $i_x = 90°$ with varying $i_y = 30°$, 60°, 90°, 120°, 150°, and 180°.

Fig. 2(b) shows analysis cases for analyzing the effect of the spacing and location of the joint on the anchorage behavior, and the influencing factors are expressed as dimensionless coefficients; i.e., spacing of rock joints (α) defined as the ratio of the joint spacing to the anchorage diameter (D) and position of rock joints (β) defined as the ratio of the position of the first joint among the joint set to the anchorage length (L). In the case of analysis on the joint spacing, β was fixed and the analyses were performed with

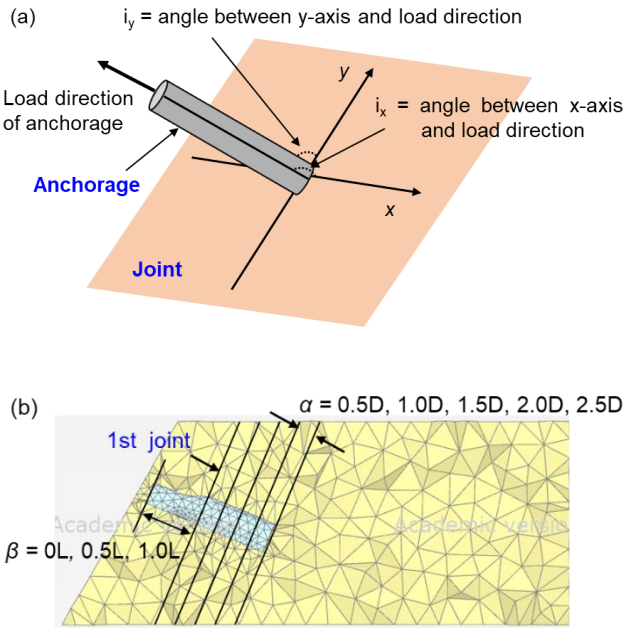

Fig. 2 Definition and key parameters: (a) effect of the direction of joints and (b) position and spacing of joints

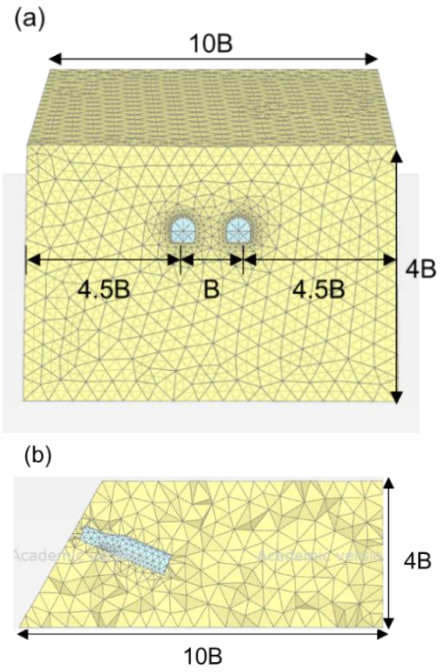

Fig. 3 Typical finite element mesh and boundary conditions: (a) front view and (b) cross section

Table 1 Cases for parametric studies

Influencing factor		Factor values	Fixed conditions
Direction of joints	i_x	0°, 30°, 60°, 90°	i_y = 90°
	i_y	30°, 60°, 90°, 120°, 150°	i_x = 90°
Spacing of joints	α	0.5D, 1.0D, 1.5D, 2.0D, 2.5D	β = 0L, 0.5L, 1.0L
Position of joints	β	0L, 0.5L, 1.0L	α = 0.5D, 1.0D, 1.5D, 2.0D, 2.5D

Table 2 Properties for the numerical studies

Material type	Unit weight (kN/m^3)	Elastic modulus (MPa)	Internal friction angle (°)	Cohesion (kPa)	Poisson's ratio
Soft rock	23	1300	37.5	100	0.25
Anchorage	17.8	28000	-	-	0.2

changing α = 0.5D, 1.0D, 1.5D, 2.0D, and 2.5D. In addition, to investigate the effect of the position of the joint on the anchorage behavior, α was fixed and the analyses was conducted with varying β = 0L, 0.5L, and 1.0L.

The range of coefficient values was appropriately analyzed by using conditions from the examples of several suspension bridges in Korea, and those were summarized in Table 1.

3. Finite element analysis

3.1 Finite element model

In this study, the pull-out behavior of tunnel-type anchorages according to the joint direction, joint spacing and position is analyzed using Plaxis 3D program (2022). Fig. 3 shows a typical model for parametric studies. The spacing between two anchorages is B, and the anchorage diameter is D. The shape of the anchorage consists of a standard part, a changing part, and a wide part. The design of the tunnel-type anchorage is rarely done in practice, thus the geometries of the tunnel-type anchorage refer to a design case of Ulsan Bridge constructed in Korea. In order to minimize the possible boundary effect of the modeling, a boundary composed of 10B in a width, 10B in a length, and 4B in a height was determined.

The soil was modeled with 10-node wedge elements while the tunnel-type anchorage was composed of 10-node tetrahedrons. The soft rock surrounding the anchorage was modeled as the Mohr Coulomb failure criteria, whereas the anchorage was modeled with linear elastic. One of the most commonly employed models in geotechnical engineering is the Mohr-Coulomb model (Jaiswal and Rakesh 2022, Das *et al*. 2022, Karira *et al*. 2022). The total number of elements in this model was from 48,765 to 137,762, depending on parameters. Table 2 shows the properties applied to numerical analyses. The model in this study consists of soft rock, joints and tunnel-type anchorage, and the properties of soft rock and anchorage refer to that of the geotechnical investigation report for Ulsan Bridge. The analysis process consisted of a total of two steps, and after implementing the geostatic stress as the first step, an external force was applied to the head of the anchorage using the load control method. At the anchorage-soft rock interface, the strength reduction factor (R_{int}) was applied to 0.67 for the soil layer and 1.0 for the soft rock to consider

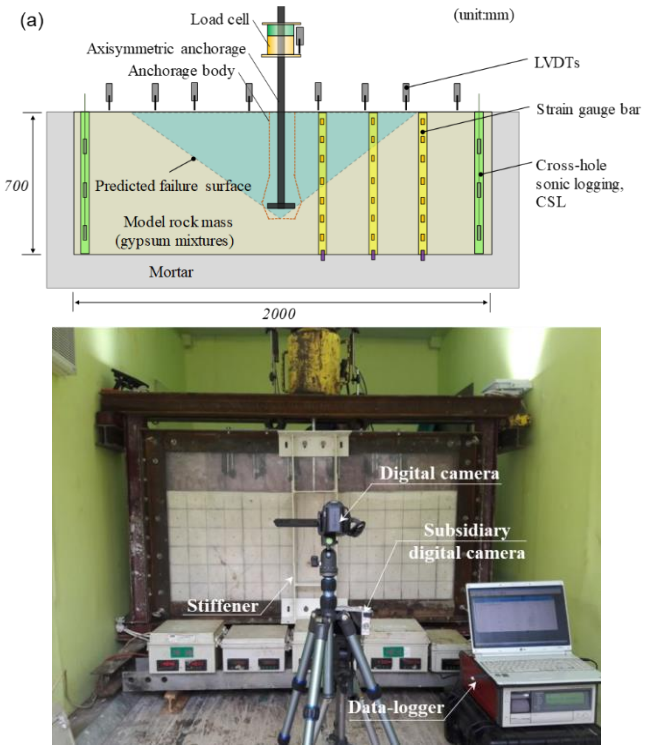

Fig. 4 2D small-scaled model test: (a) sectional view of 2D model test and (b) experimental set up (Seo *et al.* 2018, 2021)

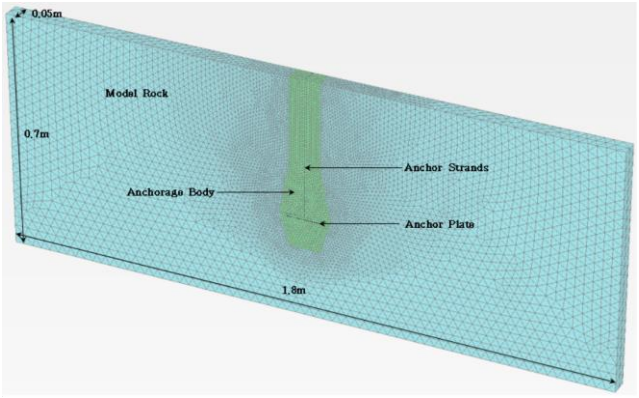

Fig. 5 Typical mesh of numerical analysis for validation

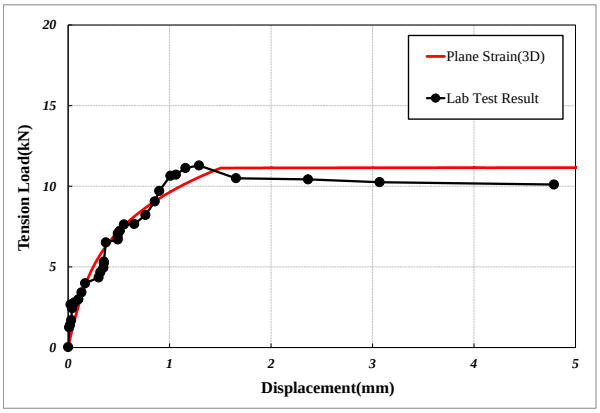

Fig. 6 Pullout load-displacement curve

the strength reduction. In addition, the rock joint was modeled as the interface. Elastic interface normal and shear stiffness values were 13.32 and 0.89 MPa, respectively. And cohesion was set to 23.5 kN/m^2, and the internal friction angle was 30.5º, based on the geotechnical investigation report for Ulsan Bridge.

3.2 Validation

The validity of the three-dimensional finite-element model was evaluated by comparing the results of the existing study (Seo *et al.* 2018, 2021). The study was conducted to analyze the failure characteristics of the tunnel-type anchorage through a small-scaled model test, and a mixture of gypsum, sand, and water was used as the material of the model ground used in the model test. The mixing ratio of the mixed materials was determined through physical property tests, and the relative strength of the actual anchorage and the surrounding ground, which reflected the similitude law, was described. Fig. 4 shows the tunnel-type anchorage two-dimensional model experiment apparatus. The model ground used in the small-scaled model test was manufactured in the size of 1,800 mm (width) × 700 mm (height) × 50mm (thickness), which corresponds to about 1/100 of the real one according to the law of physical similarity. For detailed information about the small-scaled model test, Seo *et al.* (2018, 2021) can be referred to.

Fig. 5 shows the typical mesh used in this study. The anchorage was considered as a rigid body at all times in order to prevent the local failure of the anchorage due to the cable load. For the surrounding model rock layer, the Mohr-Coulomb non-associated flow rule was adopted. The interface element modeled by the bilinear Mohr-Coulomb model was employed to simulate the anchorage-soil interface. The material properties of the model anchorage and model rock are listed in Table 2. Fig. 6 shows a comparison of the three-dimensional numerical analysis results and the load-displacement curve calculated from the test results of Seo *et al.* (2018, 2021). As shown in Fig. 6, it can be seen that the results of the 3D numerical analysis and the results of the small-scaled model test agree very well.

4. Results and discussion

In order to analyze the behavior of tunnel-type anchorage according to the conditions of rock joints, parametric studies were conducted based on variables such as the direction of joints, spacing of joints and the position of joints. The pull-out resistance-displacement curves for all influencing factors were plotted for each case to quantitatively evaluate their effects. To analyze the quantitative effect of each influencing factor on the behavior of the tunnel-type anchorage, the ratio of the pull-out resistance of each case to that of the reference case (no joint case) was defined when a displacement of 0.004L (0.4% of the anchorage length) occurred on the pull-out resistance-displacement curve, as shown in Fig. 7. In other words, the maximum value of the pull-out resistance

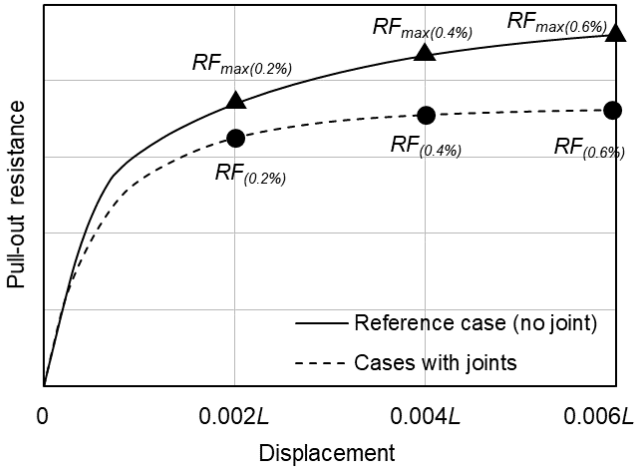

Fig. 7 Quantification of analysis results

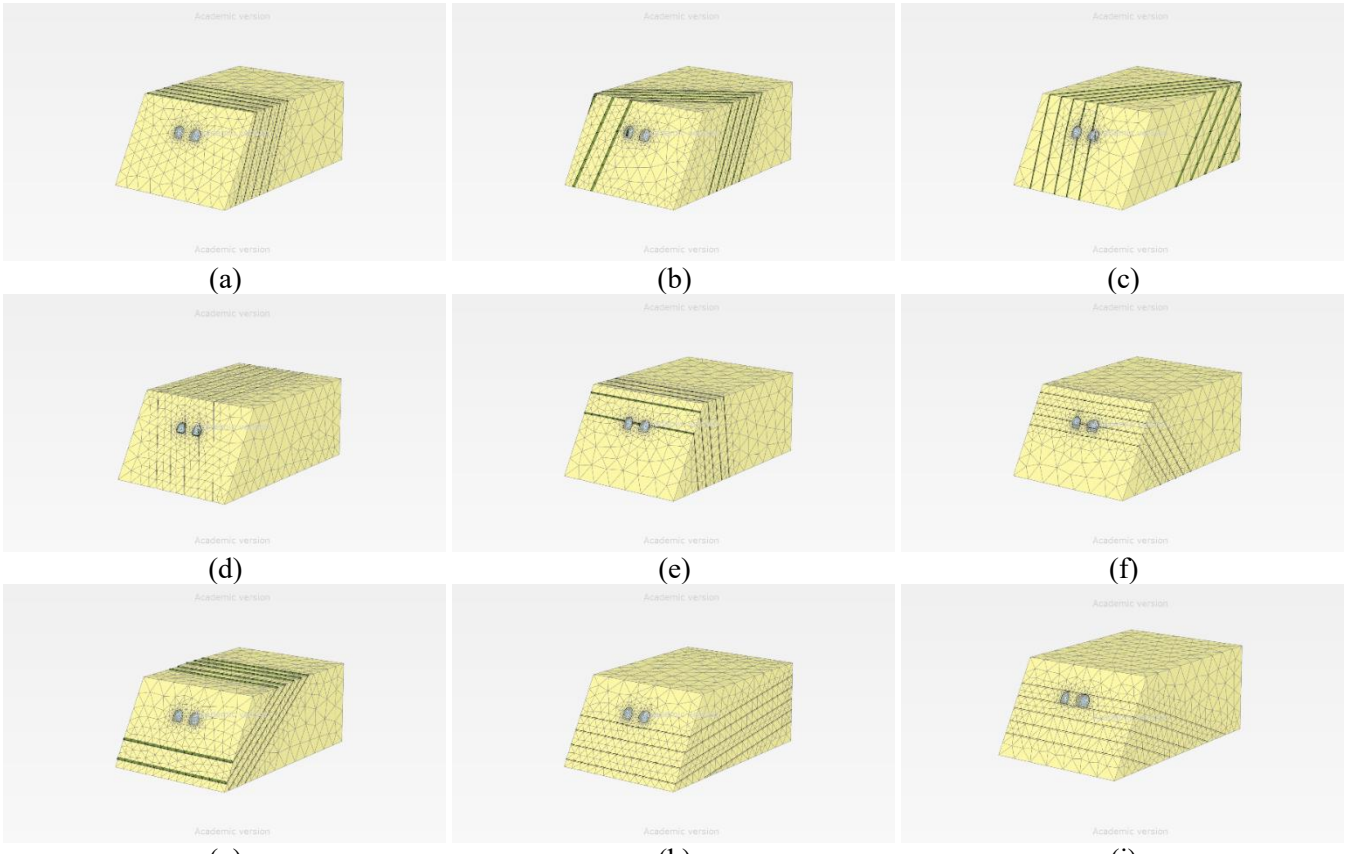

Fig. 8 Analysis cases for the direction of joints: (a) Case 1 (i_x=90°, i_y=90°), (b) Case 2 (i_x=60°, i_y=90°), (c) Case 3 (i_x=30°, i_y=90°), (d) Case 4 (i_x=0°, i_y=90°), (e) Case 5 (i_x=90°, i_y=60°), (f) Case 6 (i_x=90°, i_y=30°), (g) Case 7 (i_x=90°, i_y=120°), (h) Case 8 (i_x=90°, i_y=150°) and (i) Case 9 (i_x=90°, i_y=180°)

corresponding to a certain level of displacement in the case of no joints was determined as R_{max}, and the ratio of the pull-out resistance corresponding to the same displacement level in each case was calculated. Therefore, the effect of reduced resistance according to the joint conditions was analyzed, and the quantitative effect of each joint condition on the behavior of the tunnel-type anchorage was evaluated.

4.1 Effect of direction of joints

To analyze the effect of joint direction on the behavior of tunnel-type anchorage, a total of nine cases were analyzed (refer to Fig. 8). Cases 1 to 4 had a fixed i_y value of 90 degrees while the i_x value varied at 90, 60, 30, and 0 degrees (Figs 8(a) - (d)). Cases 5 to 9 had a fixed

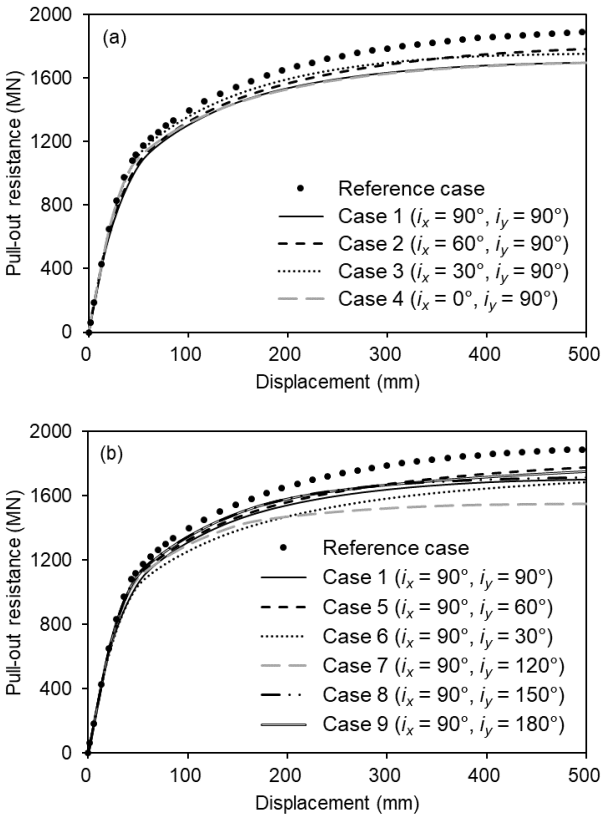

Fig. 9 Pull-out resistance-displacement curves according to the joint direction: (a) i_y = 90° and (b) i_x = 90°

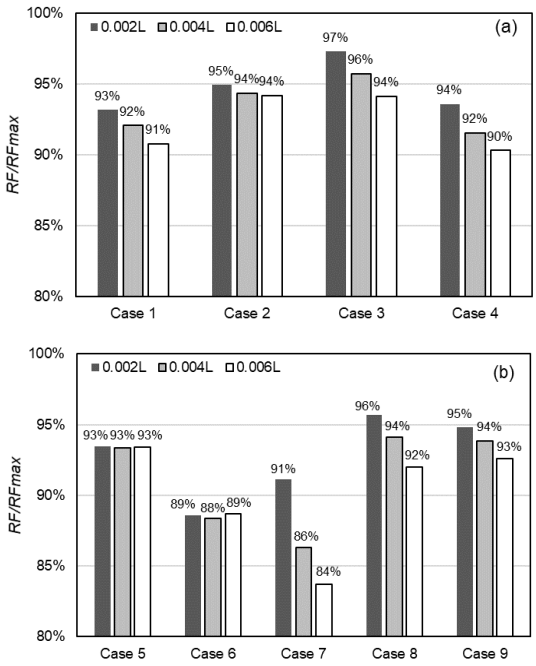

Fig. 10 RF/RF_{max} values according to the joint direction: (a) i_y = 90° and (b) i_x = 90°

i_x value of 90 degrees while the i_y value varied at 60, 30, 120, 150, and 180 degrees (Figs. 8(e)-8(i)).

Fig. 9 shows the pull-out resistance-displacement curves according to the joint direction. As shown in Fig. 9(a), Cases 1 and 4 showed the smallest pull-out resistances at the reference displacement value (0.004L = 250 mm), indicating the largest reduction in pull-out resistance due to joint effect. The results in Fig. 9(b) represent the case where i_x is fixed and i_y is varied. It can be observed that Case 7 has the smallest pull-out resistance at the reference displacement value (0.004L = 250 mm). This is because the direction of the applied load is similar to the direction where sliding may occur at the joint.

To analyze the pull-out resistance at each displacement level, the RF/RF_{max} values were plotted for each case as shown in Fig. 10. The results showed that, as shown in Fig. 10(a), Cases 1 and 4 had the smallest RF/RF_{max} value as i_x changed, and at a displacement level of 0.006L for Case 4, a decrease in pull-out resistance of approximately 10% occurred. In addition, it was found that the pull-out resistance decreased as the displacement level increased overall.

Fig. 10(b) shows the results of RF/RF_{max} as i_y changed. Unlike Cases 1 - 4, the trend of consistent decrease in RF/RF_{max} values with increasing displacement level was not observed. For Cases 5 and 6, the RF/RF_{max} values remained constant despite an increase in displacement level, while for Cases 7 - 9, the pull-out resistance decreased as the displacement level increased. Furthermore, the decrease in pull-out resistance ratio was highest in Case 7, and the reason for this is that the possibility of sliding at the joint increases due to the applied load.

When i_y is fixed at 90 degrees and i_x varies from 0 to 90 degrees, the reduction in anchorage resistance due to sliding behavior does not occur, because the effect of the slope inclination caused by the joint does not affect the direction of sliding. Fig. 11 shows the distribution of plastic points (failure) for the results of the analysis of the reference case, Case 1, Case 4 and Case 7. As shown in Fig. 11(a), in the reference case, all plastic points are distributed at the interface between the anchorage and the rock. In Case 1, it can be observed that plastic points mainly occur on the upper part of the joint surface where the anchorage passes through due to displacement caused by the applied load. This indicates that punching failure occurs depending on the direction of the load acting on the anchorage. In Case 4, as shown in Fig. 11(c), plastic points are mainly distributed in the overlapping area between anchorage and the joint surface. It indicates that the joint surface tears apart as the displacement occurs.

Case 7 has a different behavior from Cases 1 and 4. Cases 1 and 5-9 occur when i_x is fixed at 90 degrees and i_y varies, and they may have a similar direction of sliding as the load direction and the joint surface. Case 7 is the case where i_x = 90 and i_y = 120 degrees, and sliding is most likely to occur as the load is applied. As shown in Fig. 11(d), plastic points are mainly distributed at the lower part of the joint surface, indicating that the sliding behavior of the joint surface dominates when the load is applied.

4.2 Effect of position and spacing of joints

In order to analyze the effect of the position and spacing

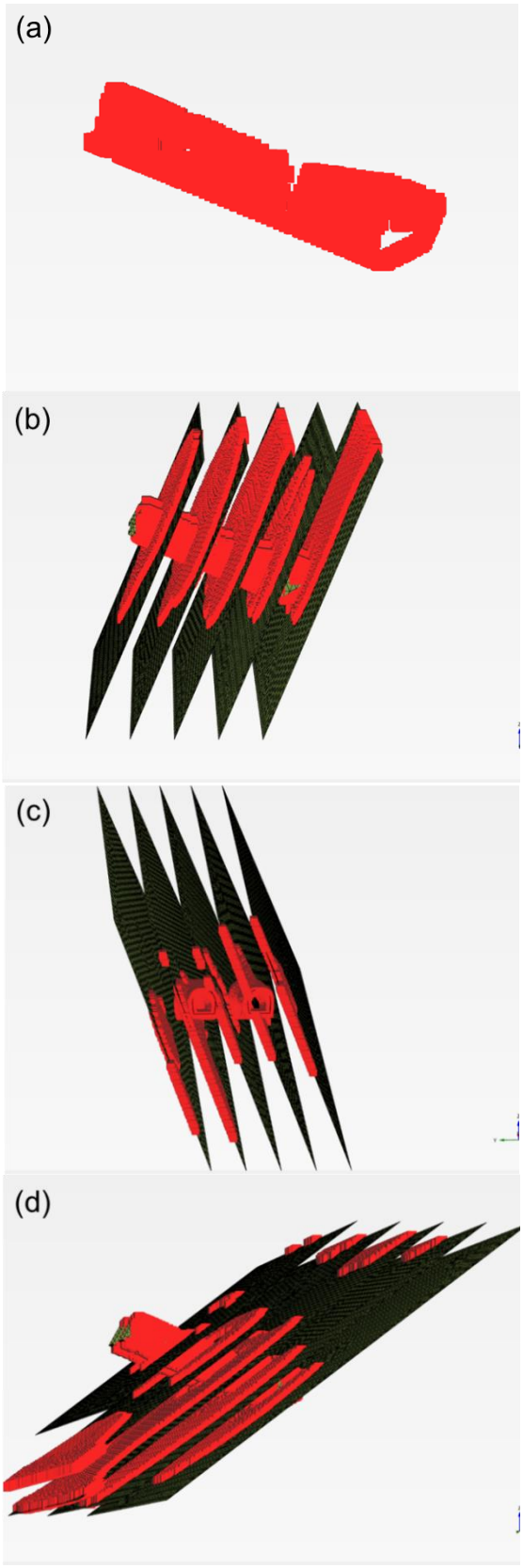

Fig. 11 Results of plastic points: (a) Reference case, (b) Case 1, (c) Case 4 and (d) Case 7 (continued)

of the rock joint on the behavior of tunnel-type anchorage, a total of 15 cases were analyzed (see Fig. 12). The analysis focused specifically on the quantitative analysis of the behavior of tunnel-type anchorage according to the position of the joint. The analysis cases were classified into three categories based on the starting position of the joints: when the joint set starts at the head of the anchorage and completely overlaps with it (0L), when the joint set starts in the middle of the anchorage and half of the anchorage overlaps with the joint set (0.5L), and when the joint set starts at the base of the anchorage and does not overlap with the anchorage (1.0L). In addition, in order to analyze the behavior of tunnel-type anchorage according to the spacing between joints, analysis cases were performed by varying the spacing between joints from 0.5D to 2.5D.

Fig. 13 shows the pull-out resistance-displacement curves for each joint spacing depending on the starting position of the joint set in tunnel-type anchorage. The cases with joint spacing between 0.5D to 1.5D (Figs. 13(a)-13(c)) had the smallest pull-out resistance values at the reference displacement (0.004L) with β = 0L, indicating that they had the greatest influence. When β = 1L, the pull-out resistance values were similar to the reference case and did not affect the behavior of the anchorage. For joint spacing of 2.0D (Fig. 13(d)), the case with β = 0L had the smallest pull-out resistance value at the reference displacement, but cases with β = 0.5L and 1L showed similar results to the reference case. Furthermore, for joint spacing of 2.5D (Fig. 13(e)), the results were similar to the reference case regardless of the starting position of the joint set at the reference displacement. This indicate that the effect of joint spacing on the behavior of anchorage decreases as the joint spacing increases and that the effect of joint spacing can be ignored when the joint spacing is 2.5D or more.

Fig. 14 is presented to quantitatively analyze the reduction in pull-out resistance of tunnel-type anchorage depending on the starting position and spacing of the joint sets. Fig. 14(a) shows the case of β = 0L where the staring position of the joint set is located at the head of the anchorage, and the entire anchorage overlaps with the joint set. As shown in the figure, it is found that the smaller the spacing between the joints, the greater the decrease in RF/RF_{max} value, indicating a significant impact on the behavior of the tunnel-type anchorage. For α = 0.5D, RF/RF_{max} is 87% for 0.002L of displacement level, RF/RF_{max} is 82% for 0.004L of displacement level, and RF/RF_{max} is 79% for 0.006L of displacement level, respectively. However, when the spacing of joints is 2.5D even with β = 0L, the RF/RF_{max} value is approximately 93~96% depending on the displacement levels, indicating that the influence of the joints on the anchorage behavior decreases as the spacing of joints increases. Fig. 14(b) shows the case of β = 0.5L where the starting position of the joint set is located at the center of the anchorage and half of the anchorage overlaps with the joint set. In this case, the RF/RF_{max} value is relatively small with a value of about 94% or more compared to the case of β = 0L. Also, as in the case of β = 0L, the impact on the behavior of the anchorage increases as the spacing between the joints decreases, but the degree of impact is not significant. Finally, Fig. 14(c) shows the case where the starting position of the joint set is located at the base of the anchorage, and the joint set does

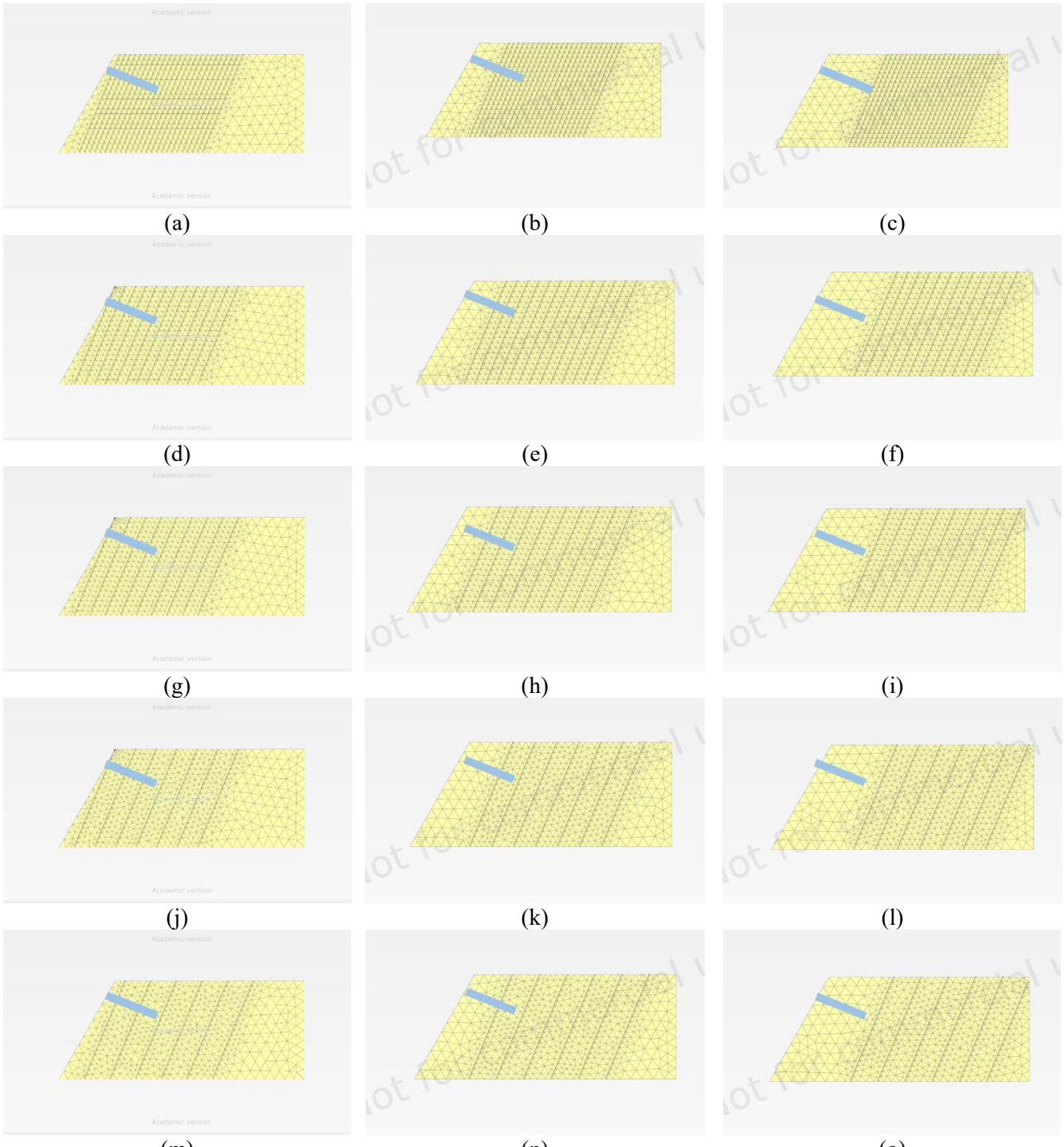

Fig. 12 Analysis cases for the spacing and position of joints: (a) Case (1) (α=0.5D, β=0L), (b) Case (2) (α=0.5D, β=0.5L), (c) Case (3) (α=0.5D, β=1.0L), (d) Case (4) (α=1.0D, β=0L), (e) Case (5) (α=1.0D, β=0.5L), (f) Case (6) (α=1.0D, β=1.0L), (g) Case (7) (α=1.5D, β=0L), (h) Case (8) (α=1.5D, β=0.5L), (i) Case (9) (α=1.5D, β=1.0L), (j) Case (10) (α=2.0D, β=0L), (k) Case (11) (α=2.0D, β=0.5L), (l) Case (12) (α=2.0D, β=1.0L), (m) Case (13) (α=2.5D, β=0L), (n) Case (14) (α=2.5D, β=0.5L) and (o) Case (15) (α=2.5D, β=1.0L)

not overlap with the anchorage. In this case, the RF/RF_{max} is about 100% for all displacement levels, indicating that the joint sets does not affect the behavior of the anchorage. Therefore, the degree of influence on the pull-out resistance of the anchorage can vary depending on the starting position and spacing of the joints. According to the results, the pull-out resistance can be reduced by about 0~21% depending on the joint condition, so it is necessary to consider this in the design stage.

Fig. 15 shows the distribution of plastic points for the

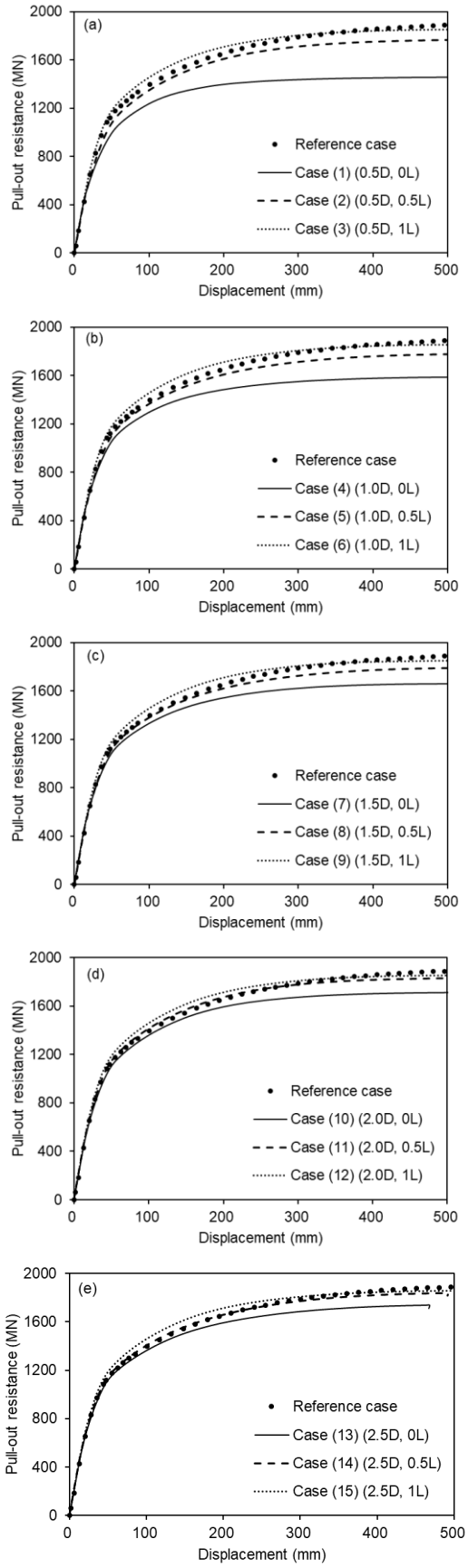

Fig. 13 Pull-out resistance-displacement curves according to the position and spacing of joints: (a) α = 0.5*D*, (b) α = 1.0*D*, (c) α = 1.5*D*, (d) α = 2.0*D* and (e) α = 2.5*D*

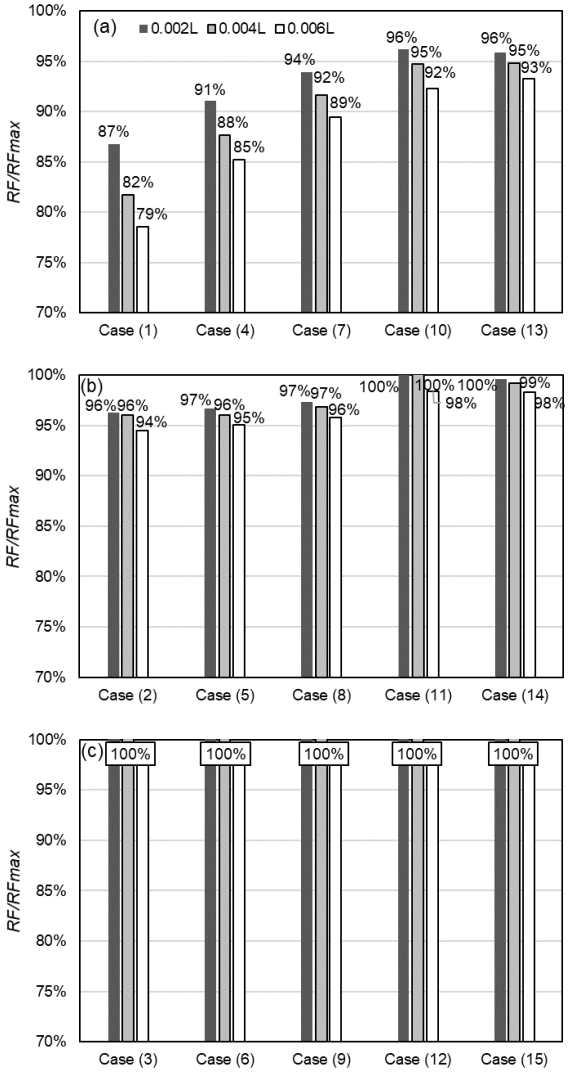

Fig. 14 RF/RF_{max} values according to the position and spacing of joints: (a) β = 0*L*, (b) β = 0.5*L* and (c) β = 1.0 *L*

analysis results of Cases (1), (2), (13) and (14). A comparison of Case (1) and Case (13), and Case (2) and Case (14), it can identify the tendency of anchorage behavior according to the joint spacing. In Case (1) and Case (13), the joint set starts from the head of the anchorage (β = 0*L*), and the joint spacing is 0.5*D* and 2.5*D*, respectively. Case (1) has 57,085 plastic points, and Case (13) has 31,616 plastic points. In addition, in Case (2) and Case (14), the joint set starts from the middle of the anchorage, and the joint spacing is 0.5*D* and 2.5*D*, and the number of plastic points is 46,143 and 25,954, respectively. Therefore, it is found that the number of joints through which the anchorage passes, the wider the area where the plastic point occurs, which leads to a decrease in the resistance of the anchorage.

Furthermore, by comparing Case (1) with Case (2) and Case (13) with Case (14), the trend of reducing anchorage resistance according to the starting position of the joint set can be analyzed. Case (1) and Case (2) have joint spacing of

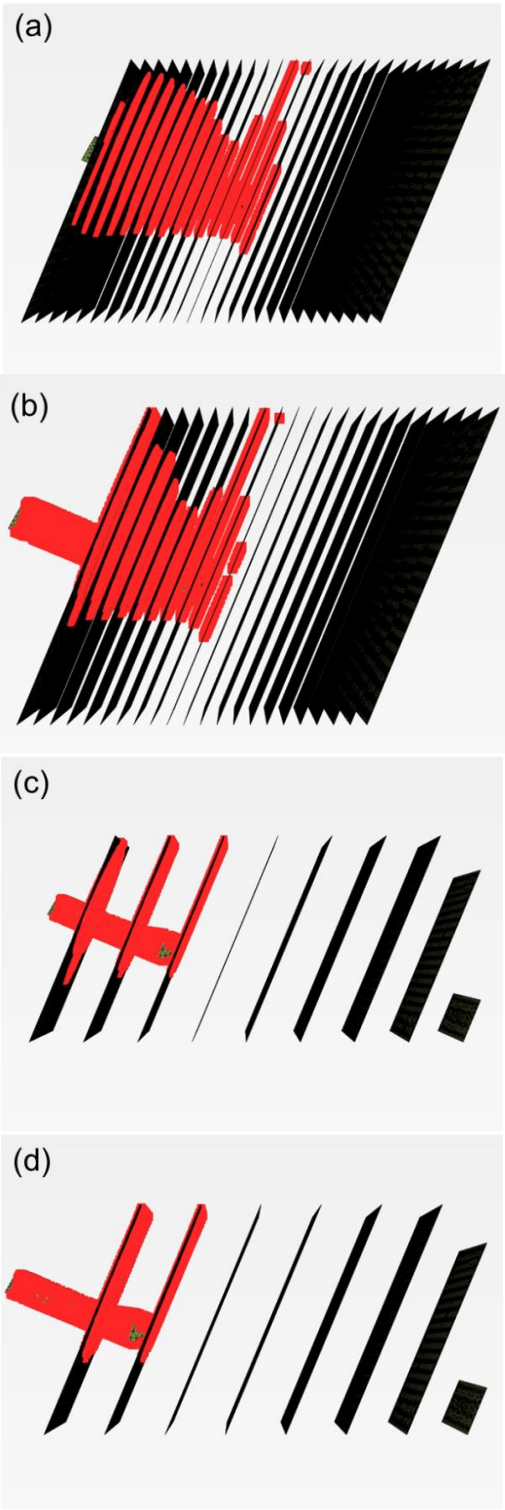

Fig. 15 Results of plastic points: (a) Case (1), (b) Case (2), (c) Case (13) and (d) Case (14) (continued)

0.5*D*, and their joint starting positions are at 0*L* and 0.5*L*, respectively. Case (13) and Case (14) have joint spacing of 2.5*D*, and their joint starting positions are at 0*L* and 0.5*L*, respectively. Comparing the plastic points of each case mentioned above, it can be observed that Case (1) and Case (13) has more plastic points than Case (2) and Case (14), respectively. It confirms that the larger the number of joint surfaces where the anchorage overlaps, the wider the area where the plastic point occurs, leading to a decrease in the resistance of the anchorage.

5. Conclusions

The study aimed to analyze the behavior of tunnel-type anchorage under varying conditions of rock joints. The direction, spacing and position of the rock joints were examined as part of the parametric studies. The emphasis is on quantifying the behavior of the tunnel-type anchorage embedded in the joint bedrock according to the joint characteristics. For the quantitative evaluation, the pull-out resistance-displacement curves were plotted for each case, and the ratio of the pull-out resistance of each case to that of the reference case was defined. The findings derived based on this study are as follows.

1. It was confirmed that the lowest pull-out resistance presented in the case where the anchorage body and the joint were perpendicular (Cases 1; i_x=90°, i_y=90°) and parallel (Case 4; i_x=0°, i_y =90°). The trend of consistent decrease in RF/RF_{max} values with increasing displacement level was not observed in Cases 5(i_x=90°, i_y=60°) and 6(i_x=90°, i_y=30°). In contrast, the pull-out resistance decreased as the displacement level increased in Cases 7-9, with Case 7(i_x=90°, i_y=120°) showing the highest decrease in pull-out resistance ratio.
2. It was found that the pull-out resistance decreased as the spacing between joints increased. The pull-out resistance decreased as the spacing between the joints increased. The RF/RF_{max} values showed that the reduction in pull-out resistance was more significant when the joint was located closer to the surface of the anchorage. When the joint was located near the surface, the anchorage had lower pull-out resistance, and the failure occurred mainly at the interface between the anchorage and the rock. However, when the joint was located deeper, the anchorage had a higher pull-out resistance, and the failure occurred mainly on the joint surface.
3. The results of the parametric studies conducted on the direction, spacing, and position of the joints can help design better anchorage systems that can withstand the challenges posed by rock joints. The study emphasizes the importance of understanding the quantitative effect of each joint condition on the behavior of tunnel-type anchorage to design and optimize the anchorage systems. The findings of the study can contribute to the development of more efficient and reliable anchorage systems in the future.

Acknowledgments

This work was supported by the National Research Foundation of Korea (NRF) grant funded by the Korea government (MSIT) (No. NRF-2022R1C1C1011477). Also, this research was supported by a grant (21SCIP-B119947-06) from the Construction Technology Research Program funded by the Ministry of Land, Infrastructure and Transport of Korean government.

References

Alawneh, A.S., Malkawi, A.I.H. and Al-Deeky, H. (1999), "Tension tests on smooth and rough model piles in dry sand", *Can. Geotech. J.*, **36**, 746–753.

ASCE (1979), "Long span of suspension bridge: history and performance", *Proceedings of the ASCE National Conventions*, Boston, MA, USA.

Aydan, Ö., Ebisu, S. and Komura, S. (1993) "Pull-out tests of rock anchors and their failure modes", In Assessment and Prevention of Failure Phenomena in Rock Engineering; CRC Press: Boca Raton, FL, USA.

Dakeuchi, K.O. and Yoshida, Y.T. (1984), "Tunnel type anchorage", Construction report of Honshousikoku connection bridge, Research Report No. **22**(11).

Das, S., Halder, K. and Chakraborty, D. (2022), "Seismic bearing capacity of shallow embedded strip footing on rock slopes", *Geomech. Eng.*, **30**(2), 123-138. https://doi.org/10.12989/gae.2022.30.2.123.

Deng, Y., Li, A., Chen, S. and Feng, D. (2018). "Serviceability assessment for long-span suspension bridge based on deflection measurements", *Struct. Control Health Monit.*, **25**(11), 1–23. https://doi.org/10.1002/stc.2254.

Gwon, S.G. and Choi, D.H. (2018). "Static and dynamic analyses of a suspension bridge with three-dimensionally curved main cables using a continuum model", *Eng. Struct.*, **161**, 250-264, 2018. https:/doi.org/ 10.1016/j.engstruct.2018.01.062.

Han, Y., Liu, X., Wei, N., Li, D., Deng, Z., Wu, X. and Liu, D. (2019). "A comprehensive review of the mechanical behavior of suspension bridge tunnel-type anchorage", *Adv. Mater. Sci. Eng.*, **2019**, 1-9. https://doi.org/10.1155/2019/3829281.

Hong, E.S., Cho, G.C., Baak, S.H., Park, J.-H., Chung, M. and Lee, S.-W. (2014), "A numerical study on pull-out behavior of cavern-type rock anchorages", *J. Korean Tunn. Undergr. Sp. Association*, **16**(6), 521-531. https://doi.org/10.9711/KTAJ.2014.16.6.521.

Ilamparuthi, K., Dickin, E.A. and Muthukrisnaiah, K. (2002) "Experimental investigation of the uplift behaviour of circular plate anchors embedded in sand", *Can. Geotech. J.*, **39**, 648-664.

Jaiswal, A. and Kumar, R. (2022), "Finite element analysis of granular column for various encasement conditions subjected to shear load", *Geomech. Eng.*, **29**(6), 645-655. https://doi.org/10.12989/gae.2022.29.6.645.

Kanemitsu, H., Omachi, T. and Higuchi, K. (1980), "Calculation method of ultimated resisting pull strength of tunnel type of anchorage for suspension bridge", *Honsi Technical Report*, **5**(16), 15-20.

Karira, H., Kumar, A., Ali, T.H., Mangnejo, D.A. and Mangi, N. (2022), "A parametric study of settlement and load transfer mechanism of piled raft due to adjacent excavation using 3D finite element analysis", *Geomech. Eng.*, **30**(2), 169-185. https://doi.org/10.12989/gae.2022.30.2.169.

Lei, J.Q., Zheng, M.Z. and Xu G.Y. (2012). Suspension Bridge Design, China Communication Press, Beijing, China.

Lekidis, V., Tsakiri, M., Makra, K., Karakostas, C., Klimis, N. and Sous, I. (2005). "Evaluation of dynamic response and local soil effects of the Evripos cable-stayed bridge using multi-sensor monitoring systems", *Eng. Geol.*, **79**(1-2), 43-59. https://doi.org/10.1016/j.enggeo.2004.10.015.

Li, J.P. and Li, Y.S. (2006). "Research on displacement of anchorage of suspension bridge", Ground Modification and Seismic Mitigation, Proceedings of the GeoShanghai Conference, Shanghai, China, June, **GSP 152**, 207-214.

Lim, H., Seo, S., Lee, S. and Chung, M. (2020). "Analysis of the passive earth pressure on a gravity-type anchorage for a suspension bridge", *Int. J. Geo. Eng.*, **11**, 1-7. https://doi.org/10.1186/s40703-020-00120-5.

Lim, H., Seo, S., Ko, J. and Chung, M. (2021). "Effect of joint characteristics and geometries on tunnel-type anchorage for suspension bridge", *Appl. Sci.*, **11**(24), 11688. https://doi.org/10.3390/app112411688.

Lim, H., Seo, S., Ko, J. and Chung, M. (2022). "Influence of geometric factors on pull-out resistance of gravity-type anchorage for suspension bridge". *Geomech. Eng.*, **31**(6), 573-582. https://doi.org/10.12989/gae.2022.31.6.573.

Park, J.W., Chung, S.T. and Cho, J.H. (2009), "The design of tunnel type anchorage in Ulsan Grand Bridge", *Yooshin technical report*, **16**, 328-336

Park, C.S., Park, J.H., Chung, M.K. and Oh, I.K. (2013), "A study for improvement of suspension bridge's tunnel anchorage design", *Proceedings of Korean Society of Civil Engineering Annual Conference*, City, Month.

Park, C.S., Park, J.H. and Chung, M.K. (2014), "Recent study for improving the calculation method of ultimate pull-out resistance of tunnel anchorage", *Proceedings of the Korean Geotechnical Society Spring National Conference*, City, 3.

PLAXIS. PLAXIS 3D Reference Manual; Bentley: Exton, PA, USA, 2022.

Seo, S., Park, J., Lee, S. and Chung, M. (2018). "Analysis of pull-out behavior of tunnel-type anchorage for suspended bridge using 2-D model tests and numerical analysis", *J. Korean Geotech. Soc.*, **34**(10), 61-74. https://doi.org/10.7843/kgs.2018.34.10.61.

Seo, S., Lim, H. and Chung, M. (2021). "Evaluation of failure mode of tunnel-type anchorage for a suspension bridge via scaled model tests and image processing", *Geomech. Eng.*, **24**(5), 457-470. https://doi.org/10.12989/gae.2021.24.5.457.

Shanker, K., Basudhar, P.K. and Patra, N.R. (2007), "Uplift capacity of single piles: Predictions and performance", *Geotech. Geol. Eng.*, **25**, 151-161. https://doi.org/10.1007/s10706-006-9000-z.

Yooshin Co., Ltd., (2009), Ulsan Grand Bridge and Access Road Private Proposal Project: Basic Design Report.

Zhang, Q., Li, Y.J., Yu, M. W., Hu, H.H. and Hu, J.H. (2015), "Study of the rock foundation stability of the Aizhai suspension bridge over a deep canyon area in China", *Eng. Geol.*, **198**, 65-77. https://doi.org/10.1016/j.enggeo.2015.09.012.

IC